Spectrochimica Acta Part A: Molecular and Biomolecular Spectroscopy 192 (2018) 473–486

Contents lists available at ScienceDirect

Spectrochimica Acta Part A: Molecular and Biomolecular Spectroscopy

journal homepage: www.elsevier.com/locate/saa

Infrared spectroscopy of flavones and flavonols. Reexamination of the hydroxyl and carbonyl vibrations in relation to the interactions of flavonoids with membrane lipids

Goran Baranović [a], Suzana Šegota [b,*]

[a] Division of Organic Chemistry and Biochemistry, R. Bošković Institute, Zagreb, Croatia
[b] Division of Physical Chemistry, R. Bošković Institute, Zagreb, Croatia

ARTICLE INFO

Article history:
Received 22 September 2017
Received in revised form 18 November 2017
Accepted 25 November 2017
Available online 02 December 2017

Keywords:
Flavone
Flavonol
Vibrational assignment
Infrared spectrum
Raman spectrum
B3LYP/6-31+G(d,p) level of theory

ABSTRACT

Detailed vibrational assignments for twelve flavonoids (seven flavones (flavone, 3- and 5-hydroxyflavone, chrysin, apigenin, fisetin and luteolin) and five flavonols (galangin, kaempferol, quercetin, morin and myricetin)) have been made based on own and reported experimental data and calculations at the B3LYP/6-31+G(d,p) level of theory. All the molecules are treated in a uniform way by using the same set of redundancy-free set of internal coordinates. A generalized harmonic mode mixing is used to corroborate the vibrational characteristics of this important class of molecules. Each flavonoid molecule can be treated from the vibrational point of view as made of relatively weakly coupled chromone and phenyl part. It has been shown that the strongest band around 1600 cm^{-1} need not be attributable to the C═O stretching. The way the vibrations of any of the hydroxyl groups are mixed with ring vibrations and vibrations of other neighboring hydroxyl groups is rather involved. This imposes severe limitations on any attempt to describe normal modes of a flavonol in terms of hydroxyl or carbonyl group vibrations. The role of water molecules in the appearance of flavonoid IR spectra is emphasized. Knowing for the great affinity of phosphate groups in lipids towards water, the immediate consequence is a reasonable assumption that flavonoid lipid interactions is mediated by water.

1. Introduction

It is well known that important and multipurpose role of flavonols in maintaining the human health is closely related to their ability to act as a scavenger of free radicals that are normally produced on the course of numerous metabolic reactions. The interactions of flavonoids with membranes or, more specifically, with membrane lipids make a distinctive part of this complicated picture [1]. It has emerged that the main structural reason lies in the hydroxyl groups attached to the various position of the ring structures. The structural characteristics that are presumably most important are thus the hydroxylated B-ring (Fig. 1), and the presence of the double bonds C2═C3 and C═O in C-ring. The hydroxyl groups of B ring are the most important factor in scavenging of radical species. The 4-oxo group of C ring is an accepting part of up to two intramolecular hydrogen bonds. It is generally thought that these parts contribute significantly to the stability of the flavonoid radicals [2].

The main motivation for this work is to achieve a uniform interpretation of the vibrational spectra of a selected group of flavones and flavonols based on experimental and theoretical results as a prerequisite for better understanding of the changes in their IR spectra when they are adsorbed on or built in lipid bilayers, i.e. liposomes. By monitoring spectral changes brought about by lipid flavonoid interactions it should be possible to reveal structural details of how the flavonoids incorporate onto or into the lipid bilayer. As is well known flavonols are at best sparingly soluble in water and buffers and somewhat better soluble if small quantity of alcohol is added. Generally, methanol and/or ethanol are the only suitable pure solvents for obtaining solution IR spectra of flavonols. No wonder that behavior of flavonols and flavones (and other flavonoids) depends strongly on pH of the surrounding [3]. Therefore in obtaining experimental vibrational data one is practically limited to the vibrational spectra of solid flavonoids.

An important characteristic of a flavonoid molecule with respect to its interactions with membranes is its hydrophobicity. It is generally accepted that hydrophobic flavonoids can be built in and even cross the lipid bilayer. The less hydrophobic flavonoids are more likely to be adsorbed via binding with the polar headgroups of lipids at the lipid-water interface [1]. Although IR spectroscopy evidently is much used in elucidating interactions of flavonoids with membrane lipids [4,5,6] the conclusions drawn from IR spectra about the way flavonoids are incorporated onto or into lipid bilayers are rather vague and are generally not far reaching. The main reason lies in the fact that the actual state in which the flavonoid molecules are bound to lipids in a buffer solution is not known. When quercetin is observed in interaction with lipids, it

* Corresponding author.
E-mail address: ssegota@irb.hr (S. Šegota).

https://doi.org/10.1016/j.saa.2017.11.057
1386-1425/

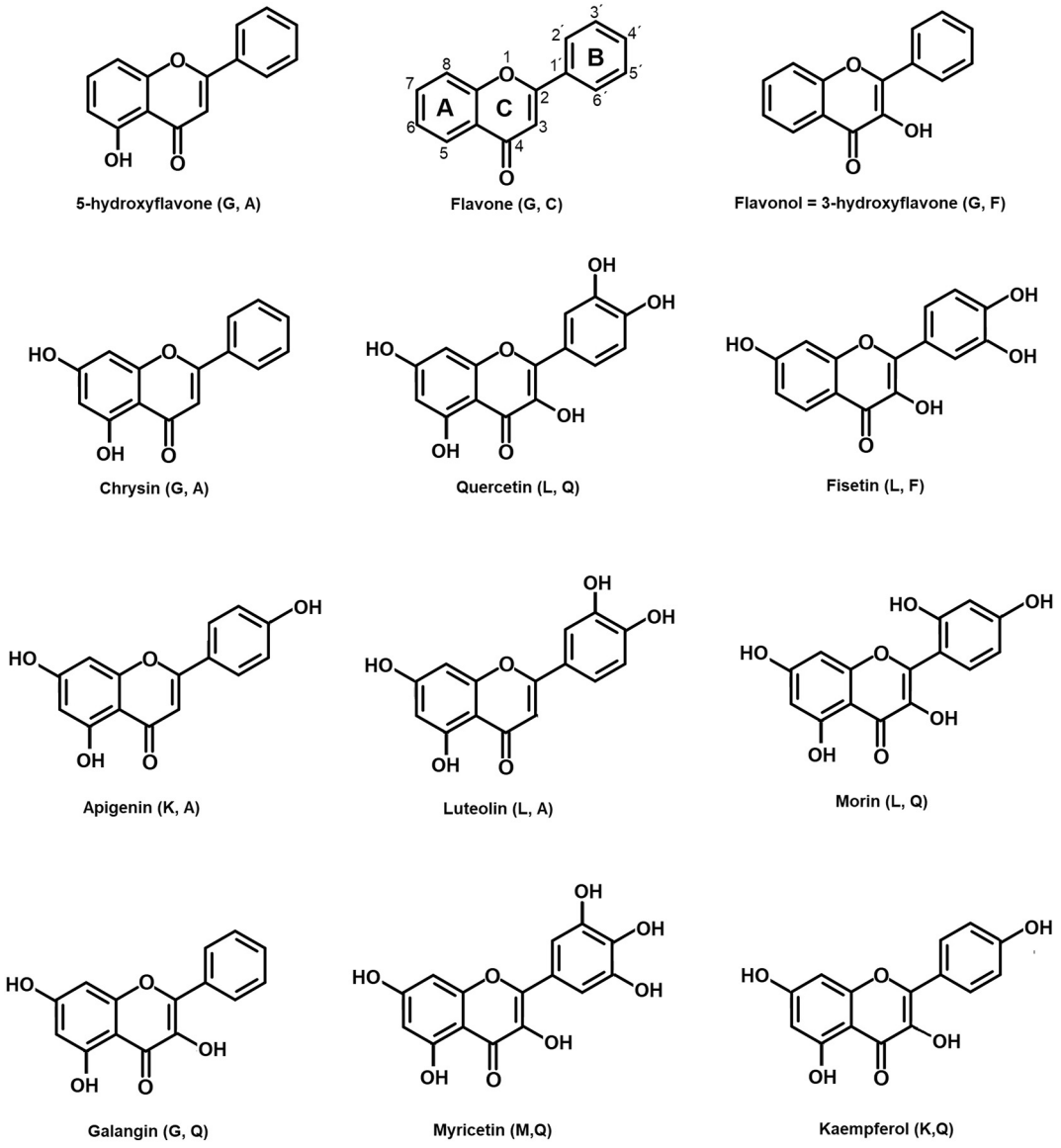

Fig. 1. Molecular diagrams and atom numbering (symbols in parentheses are defined in Table 1).

should be possible to confirm the essential role of hydroxyl groups in adsorption and incorporation within the lipid bilayer. The stability of flavonoid molecules is strongly dependent on pH and less so on the temperature. For example, myricetin is more stable in acidic than in basic conditions. It degrades quickly at pH 7.4 and thus would lose its activity practically immediately after entering the bloodstream. It is reasonably stable at body temperature [7]. The next related and equally important question is whether an anion or a neutral flavonoid molecule is observed within the time interval (typically a few hours) of its stability under given pH and temperature. Therefore an attempt to identify the corresponding parts of IR spectra of flavonols seems highly desirable. However, the reliable assignment of IR or Raman vibrational spectra is hard to achieve because of the flavonoid vibrational characteristics that will be discussed later on.

It is very convenient, as it will become clearer later, to group the studied compounds as shown in Table 1 (also in Tables S1 and S2). In columns are the groups defined by the 4-oxo group surrounding. In rows are the groups having the same number of hydroxyls on B-ring. Whatever way of grouping is chosen it is always be possible to find a pair of molecules differing in the number of hydroxyl groups by one only. Hopefully, this will be very helpful in assigning the spectra of a more complex molecule.

The literature survey with respect to vibrational studies of flavones and flavonols and their physical properties presents rather active field of research. From the reported data it is quite obvious that vibrational analysis of any flavonoid is not straightforward because of at least two problems, i.e. (i) the conformational preference problem and (ii) the presence of rings that ensure non-negligible couplings even between distant internal oscillators. In the detailed conformational analysis of quercetin performed at the B3LYP/6-31G(d,p) level of theory as many as 12 conformations of quercetin molecule with relatively small Gibbs energy differences from 0 to 5.33 kcal/mol were described [8]. The presence of relatively strong intramolecular hydrogen bonds in the quercetin molecule was shown to substantially lower the molecular energy. For the two lowest energy conformations the dihedral angle θ between the C- and B-ring is either 0 or 180°, i.e. they are planar. In the crystal of dihydrate $\theta = 7°$ which is definitively due to the packing reasons [9], while in the crystal of monohydrate quercetin molecule is again planar [10]. That the flavonols (quercetin, myricetin and galangin, all in group **Q** (Table 1)) are planar was also obtained at the B3LYP/6-31G(d,p) level of theory [11]. A series of 17 flavone derivatives, flavonoids, was analyzed through a systematic B3LYP/6-311++G(d,p) computational study with the aim of understanding the molecular factors that determine their structural and energetic properties in gas phase [12].

Table 1
Studied flavonoids according to the positions and number of hydroxyl groups.

Group	**C**—	**F** 3-OH	**A** 5-OH	**Q** 3,5-OH
G—	Flavone (S7)[a]	3-Hydroxyflavone (S8)	5-Hydroxyflavone (S9), chrysin (S10)	Galangin (S11)
K 4′-OH			Apigenin (S13)	Kaempferol (S14)
L 3′,4′-OH		Fisetin (S16)	Luteolin (S17)	Quercetin (S8), morin[b] (S19)
M 3′,4′,5′-OH				Myricetin (S21)

[a] Flavone is fully described in Table S7, 3-hydroxyflavone in Table S8, etc.
[b] 2′,4′-OH.

Molecular planarity of the studied molecules is determined by the presence of C3—OH group that takes part in a weak hydrogen bonding with C6′—H atom in B-ring. In order to avoid the problem of conformational preference it was assumed in the present paper that in a given flavonoid molecule all possible intramolecular hydrogen bonds are present [13]. Even in such a case the choice is not unique because by rotating the B-ring around the inter-ring C2—C1′ bond by 180° another conformation (*syn* or *anti* with respect to the carbonyl) with not much different energy is generated. Nevertheless, only one of the two will be here fully treated. Support to this attitude is provided by experimentally unresolvable similarity of the spectra of the two conformers. In addition, since only the spectra of flavonoid crystalline or powdered samples are here studied, the observed bands are most often due to a single conformer that is present in the crystal. Except flavone with two molecules per asymmetric unit [14], other crystals have one molecule pre asymmetric unit (3-hydroxyflavone [15], quercetin [9,10], myricetin [16]).

Group **F** flavonoids (Table 1) are planar. 3-Hydroxyflavone and related flavone and 5-hydroxyflavone were very attractive subject of research because of the fast excited state proton transfer that enables dissipation of the electronic excitations into heat. It has been demonstrated that the nature of intramolecular hydrogen bonding provides an understanding of their unusual excited state. The correct vibrational assignment of the ground-state structures was therefore essential, especially for the C═O bond stretching. For argon-matrix isolated 5- and 3-hydroxyflavone the bands at 1660 and 1652 cm^{-1} were assigned to the carbonyl stretching, respectively [17]. In more recent study it has also been demonstrated by calculations at the B3LYP/6-31 + G(d) level that the bands 1619 and 1562 cm^{-1} involve the C═O stretching and the C2═C3 stretching of the pyrone ring [18]. In the gas phase the C═O stretching of flavone is at 1683 cm^{-1} [19]. It is significantly downshifted by 20 cm^{-1} in 3-hydroxyflavone and 30 cm^{-1} in 5-hydroxyflavone. A vibrational study of fisetin by means of experimental IR and Raman spectroscopies and DFT calculations at the M05-2X/6-311 + G (2df, p) level also revealed significant coupling between C═O and C2═C3 stretchings of C-ring [20].

Group **A** molecules (5-hydroxyflavone, chrysin, apigenin, luteolin) are non-planar. Intramolecular hydrogen bond in this group is much stronger than in group **F** (six-membered ring vs. five-membered ring) and the normal modes with partial C═O stretching character are found at lower wavenumbers. The only difference between luteolin and fisetin is in the position of the OH group (Table S1) that is involved in hydrogen bonding with carbonyl oxygen. This is enough to produce profound difference in their IR and Raman spectra in the 1750–1400 cm^{-1} region [13].

Group **Q** molecules (galangin, kaempferol, quercetin, morin, myricetin) are all planar except morin. With an OH substitution at position 2′ and consequently with a possibility of an additional intramolecular hydrogen bond morin molecule is non-planar. Raman and SERS spectra of quercetin were studied and compared with those of flavone, 3- and 5-hydroxyflavone [18]. Raman spectra of quercetin in solid state and in methanol solution are also reported [21]. Calculated (MP2/6-31G(d)) IR spectra of not only quercetin but also apigenin, catechin and fisetin are available [22] along with the list of the intervals of experimental frequencies within which some groups of vibrations are to be found, although not much can be extracted therefrom. A detailed vibrational study of myricetin and its O-glycoside derivative myricitrin with emphasize on the intramolecular hydrogen bonding (as a decisive factor determining the structure of the O-glycoside derivative) has been published recently [23]. A conformational and vibrational analysis of a series of flavonols, among them chrysin, fisetin and luteolin, was performed by DFT calculations (B3LYP/6-31G(d,p)) [13]. Two structural aspects were emphasized, namely, intramolecular hydrogen bonds and catechol-like B-ring. It was also pointed out that fisetin was studied in its hydrated form i.e. under the condition that are much different from those assumed in calculations.

To summarize, vibrational spectra of flavones and flavonols require uniform and more detailed analysis with respect to their relation to the molecular structural properties. In this paper we are dealing with flavonols in their biologically not important states (as solids or dissolved in organic solvents, i.e. not in water) which, however, is an important prerequisite for understanding their spectra in buffers and in interactions with, for example, lipids. It is our goal to establish a uniform point of view on the vibrational spectra of flavonols starting from flavone having no hydroxyl group and then follow the spectral changes brought about by introducing hydroxyl groups. General vibrational characteristics of the selected flavonoids will be pointed out according to the assumed groupings (Tables 1, S1, S2). The comparative vibrational analysis will be performed in four ways:

(I) Vibrational assignments for three flavonols, kaempferol, quercetin and myricetin, with increasing number of hydroxyl groups on B-ring will be presented. At the end this analysis may lead to the conclusions about the overall performances of the B3LYP/6-31 + G(d,p) model.

(II) Observed and calculated spectra of flavonoids grouped into groups **G**, **K**, **L** and **M** formed according to the substituents on B-ring (Tables 1 and S1) will be subsequently compared. This is necessary because of the exceptional role that the hydroxyl groups on B-ring have in the scavenging ability of flavonols. Hydroxyl groups participating in intramolecular hydrogen bonds will also be here discussed.

(III) It can be shown that the characteristics of the carbonyl stretching C═O are clearly displayed by grouping the flavonols according to intramolecular hydrogen bonds to carbonyl oxygen (groups **F**, **A** and **Q**, Tables 1 and S2). Measured and calculated spectra for a selected flavonoid or for a group of flavonoids will be analyzed by means of the contributions of individual internal oscillators to the potential energy paying particular attention to the C2═C3 and C═O stretchings in C-ring.

(IV) Our goal is also to solve the problem of spectral interpretation by applying an approach that will enable to decipher the spectrum of a flavonol in terms of the spectrum of another flavonoid simpler than the first one in some sense. The way how to do it has been described and is known under the name of generalized harmonic mode scrambling (mixing) analysis [24]. It will emerge that there is a difference in the normal mode characterization based on the potential energy distribution and Cartesian displacements. In the harmonic mode mixing analysis Cartesian displacements of the normal modes are compared. The necessary condition for a such comparison is the possibility to bring the smaller molecule in coincidence with a corresponding part of

the bigger molecule. Vibrational modes of complex molecules can thus be explained by the modes of the simpler molecules. For example, benezene, phenol, catechol (1,2-dihydroxybenzene) or pyrogallol (1,2,3-trihydroxybenzene) can be used to locate vibrations of B-ring in chrysin, kaempferol, quercetin and myricetin, respectively. In full analogy with the case of benzene derivatives, flavone can be used as a reference molecule for all molecules here studied (Table 1). The net result of the harmonic mode mixing analysis performed on, for example, (catechol, quercetin) pair will be more or less clear designation of the quercetin spectrum where the hydroxyl groups C2′— and C3′—OH groups contribute.

2. Experimental and Calculations

Kaempferol (>90% (HPLC), powder), quercetin (>95%, solid), myricetin (>96%, crystalline) were purchased from Sigma-Aldrich and used without further purification. IR spectra of solid samples were recorded on a Bomem MB102 FTIR spectrometer by accumulating 60 scans and at 4 cm^{-1} nominal resolution. The samples were in the form of KBr pellets for transmission measurements or minute quantities of pure substances for single reflection ATR measurements on a Specac Golden Gate accessory.

All the molecular geometries and frequencies were calculated at the B3LYP/6-31 + G(d,p) level of theory using Gaussian09 suite of programs [25]. The choice of this particular level was made after considering the results in [26]. Taking into account its performances together with the size of the molecules and their number, the selected theoretical method is an optimum one. Its quality was additionally confirmed by its ability to very successfully predict not only wavenumbers, but also intensities of phenol, catechol and pyrogallol (Tables S12, S15 and S20, respectively). To easy the comparison between calculated and observed wavenumbers a quadratic scaling method was used [27].

$$\tilde{\nu}_{scaled} = \tilde{\nu}_{calc} * (1 - 0.00001356 * \tilde{\nu}_{calc})$$

(derived for the same functional, but for a slightly different basis set, 6-311G(d,p)). Since for empirically well established assignments of phenol, catechol and pyrogallol, the average deviation of the scaled calculated wavenumbers from the observed wavenumbers was 3–4% accompanied with reasonable agreement in intensities, when assigning the spectra of presently studied molecules it seems reasonable to keep the average deviation within ± 10 cm^{-1}.

By using appropriate linear combinations of elementary (basic) internal coordinates it was possible to define non-redundant sets of internal coordinates [28] (Table S3). Only sets of internal coordinates free of both local and cyclic redundancies are suitable for comparison of force constant values between different similar molecules. The same set of non-redundant internal coordinates was thus used throughout making comparison of the force constant values between different molecules fully justified. The fractional contribution to the energy of the i-th normal mode (potential energy distribution (P.E.D.)) from the diagonal terms of the potential energy matrix **F** were calculated according to

$$L_{ji}{}^2 F_{jj}/\lambda_i$$

where L^{-1} is a transformation from internal to normal coordinates and λ_i is proportional to the wavenumber squared of the i-th normal mode [29]. Since the contributions of the non-diagonal elements (that can be negative) are also evaluated, the fractional contributions from the diagonal terms are not percentages. The normal coordinate analysis was performed using a set of programs that includes automatic generation of internal and symmetry coordinates for a given molecular structure developed by one of the authors (G. B.). The set of programs has grown by modifying and upgrading Schachtschneider's programs [30, 31].

3. Results and Discussion

3.1. Vibrational IR Spectra of Kaempferol, Quercetin and Myricetin

When any of the flavonols interact with its surroundings it is very probable that the observed spectral changes will be related to the hydroxyl and carbonyl group vibrations. These six + three vibrations are OH and CO stretchings (OH and CO, respectively), CO in-plane (COip) and out-of-plane (COop) bendings, COH bending (COH), torsion around CO bond (tCO), C═O stretching (C═O), C═O in-plane (C═Oip) and C═O out-of-plane (C═Oop) bendings. At first guess it might be reasonable to expect that the recognition of the spectral intervals occupied by these vibrations is going to be the most useful result of this study. However, except for the OH and C═O stretchings other wanted intervals seem to be ill defined. The way the vibrations of any of the hydroxyl groups are mixed with ring vibrations and vibrations of other neighboring hydroxyl groups is rather involved. This imposes severe limitations on any attempt to describe normal modes of a flavonol in terms of hydroxyl or carbonyl group vibrations.

In order to estimate the quality of the B3LYP/6-31 + G(d,p) level of theory on which more general conclusions on the vibrational spectroscopy of flavonols are to be based, the experimental data for kaempferol, quercetin and myricetin will be used. Together with galangin they belong to the groups (**Q**, **G**), (**Q**, **K**), (**Q**, **L**) and (**Q**, **M**) (Table 1). The chosen series of flavonols is very suitable for observing the spectral changes upon introducing an additional hydroxyl group to the B ring, leaving the chromone part unchanged. Observed and scaled calculated wavenumbers along with the detailed assignment according to the potential energy distribution (PED) are given in Tables 2, 3, and 4, respectively. It has turned out that the chosen model predicts quite satisfactorily not only wavenumbers, but IR intensities as well (Figs. 2, 3, and 4). When only calculated spectra of galangin, kaempferol, quercetin and myricetin are plotted (Fig. S1) it is easily seen what spectral changes accompany the increase of the number of hydroxyls. That is not possible when observing only the measured spectra (Fig. S2) because, obviously, other differences exist besides the number of hydroxyls. Therefore, the following comparative analysis of flavonol IR spectra will refer to the calculated spectra in an attempt to extract their full characterization.

An interesting observation is that all transitions below 1000 cm^{-1} are of much lower intensity, i.e. the bands in the region 1800–1000 cm^{-1} dominate IR spectra of kaempferol, quercetin and myricetin [13]. The pattern seen below 1000 cm^{-1} is populated with out-of-plane vibrations that are generally of lower intensities and is also a consequence of interactions between first neighbors in the crystal phase. This is of practical importance in experiments with lipids because only the bands above 1000 cm^{-1} can be observed with certainty taking into account the limitations inherent to IR spectroscopy technique. Therefore, in the following only the region 1800–1000 cm^{-1} will be analysed in more details.

Comparing kaempferol (Table 2, Fig. 2) with galangin (Table S11, Fig. S2) new bands introduced by a hydroxyl group at the 4′ position are close to those of the C7—OH group, but also of the C3—OH and C5—OH groups, although the latter two participate in intramolecular hydrogen bonds. For example, a medium strong band at 1276 cm^{-1} (calculated at 1280 cm^{-1}) is assigned to the C4′—O stretching, a very strong band at 1176 (1168) cm^{-1} to C4′—OH bending etc. The five strongest observed bands (with assigned calculated values in parenthesis) of kaempferol (Fig. 2) are at 1662 (1654), 1614 (1618), 1508 (1504), 1383 (1379) and 1176 (1168) cm^{-1} and they are described as CC stretchings of **A**-ring, C2═C3 stretching, CC stretching and CH in-plane bendings of **A**-ring, C3—OH bending and COH bendings in B- and A-ring, respectively. The C═O stretching bands at 1600 (1603) and 1570 (1570) cm^{-1} are not among the five strongest. Other strong bands at 1508, 1383 and 1176 cm^{-1} are attributed to A ring in-plane deformations, C3—OH bending and C5—O stretching and C4′—OH and/or

Table 2
Observed IR and scaled wavenumbers of kaempferol.

Kaempferol					
Observed	Qi[a]	Scaled	Pot. energy distrib[b,c]		
–	Q1	3626 w	99 **A**OH7		
3420 vs bd	Q2	3624 w	99 **B**OH		
3313 vs sh	Q3	3428 w	99 **C**OH		
3212 vs sh	Q4	3185 m	98 **A**OH5		
–	Q5	3116 vw	99 **B**CH		
–	Q6	3098 vw	99 **A**CH		
–	Q7	3095 vw	92 **B**CH		
–	Q8	3070 vw	92 **B**CH		
–	Q9	3060 vw	100 **A**CH		
–	Q10	3036 vw	99 **B**CH		
1662 vs	Q11	1654 s	25 **A**CC	16 **A**CC	
1655 sh	Q12	1631 vw	36 **C**CCd		
1614 vs	Q13	1618 m	18 **C**CCd	16 **B**CC	15 **B**CC
1595 s sh	Q14	1603 vs	23 **C═O**	20 **A**CC	13 CCf
–	Q15	1588 vw	26 **B**CC	20 **B**CC	14 **B**CC
1570 s	Q16	1570 w	32 **C═O**	16 **A**CC	13 **A**CC
–	Q17	1518 w	15 **B**CHip	15 **B**CHip	13 **B**CHip
1508 s	Q18	1506 m	15 **A**CC	15 **A**CHip	11 **A**CC
1485 sh	Q19	1484 m	21 **A**COH5	14 **C**CC	11 **C═O**
1458 m	Q20	1447 vw	13 **B**CC	11 **B**CC	
1438 m	Q21	1433 vw			
–	Q22	1406 vw	29 CCf	22 **A**COH5	21 **A**CC
1383 s	Q23	1379 m	16 **C**COH	16 **A**CO5	15 **A**q12
–	Q24	1353 vw	18 **B**COH	18 **B**CHip	16 **B**CHip
–	Q25	1338 vw	30 **A**CC	14 **A**CC	13 **C**CC
1317 s-	Q26	1323 m	40 **C**COH	32 CCir	
1304 s	Q27	1315 vw	19 **B**CC	16 **B**CC	14 **B**CHip
1276 m	Q28	1280 w	53 **B**CO		
–	Q29	1265 m	14 **C**CC	14 **A**CC	13 **A**COH5
1254 s		–			
–	Q30	1242 vw	29 **A**COH7	18 **C**COr	
1225 s	Q31	1213 w	22 **C**CO	21 **C**COr	
1194 m	Q32	1189 w	19 **B**CHip	11 **B**CHip	
1183 sh	Q33	1182 vw	27 **A**CHip	13 **A**CO7	
1176 vs	Q34	1168 m	59 **B**COH	13 **B**CHip	13 **B**CC
–	Q35	1160 s	38 **A**COH7	22 **A**CHip	
1130 w	Q36	1132 vw			
–	Q37	1123 vw	11 **B**CHip		
1090 m	Q38	1091 vw	26 **C**COr		
–	Q39	1016 vw	26 **B**q12	11 **B**CC	
1009 m	Q40	1011 vw	12 **B**q12	11 **A**CC	11 **A**CC
976 m	Q41	981 vw	17 **A**q12		
–	Q60	968 vw	52 **B**CHop	33 **B**CHop	28 **B**CHop
–	Q61	952 vw	66 **B**CHop	26 **B**CHop	22 **B**q4
885 m	Q42	883 vw	16 **C**q12		
849 m		–			
835 w	Q62	840 vw	59 **B**CHop	32 **B**CHop	17 **B**CHop
–	Q43	825 vw	19 **B**CO	16 **B**q12	14 **B**q6a
–	Q63	825 vw	54 **A**CHop	54 t**A**CO5	
818 m	Q64	813 vw	55 **B**CHop	23 **A**CHop	17 **B**CHop
–	Q65	811 vw	81 **A**CHop	16 **B**CHop	11 **A**q16b
796 m	Q66	803 w	64 **A**CHop	35 t**A**CO5	27 **A**q4
748 w bd		–			
723 w	Q67	717 vw	90 **C═O**op	72 tCCf	51 **C**q4
–	Q44	713 vw	25 **C**q12		
704 w	Q68	706 vw	115 **B**q4	32 **C**q4	32 **B**CCir
–	Q45	685 vw	18 **A**q12		
676 w bd	Q69	665 vw	109 **A**q4	61 **A**CO7o	41 tCCf
–	Q46	647 vw	66 **B**q6b		
–	Q47	638 vw	17 **A**q6b	12 CCf	12 **C═O**ip
–	Q70	634 vw	103 **A**CO7op	43 **A**q4	42 **A**q16b
621 w	Q71	620 vw	60 **C**q4	38 **C**CCir	19 t**C**CO
611 sh	Q72	601 vw	36 t**C**CO	25 **A**CO7op	25 **A**q16a
–	Q73	591 vw	45 t**C**CO	22 **A**CO7op	18 **C**CCir
586 w	Q48	585 vw	17 **A**q6a	11 **A**q12	
567 vw	Q49	567 vw	28 **B**q6a	16 **C**q6a	15 **A**CO5ip
521 vw	Q50	522 vw	31 **A**q6a	26 **A**q6b	25 **C**q6b
497 w	Q74	501 vw	55 **B**COop	52 **B**q16a	25 **B**CCir
460 vw	Q51	459 vw	20 **C**q6b	13 **C**q6a	
–	Q52	434 vw	57 **B**COip	19 **B**q6b	17 **B**CCir
411 w	Q75	413 vw	174 **B**q16b	11 **B**CHop	
–	Q53	400 vw	23 **A**q6b	15 **A**CO5ip	13 **C**q6a

(continued on next page)

Table 2 (*continued*)

Kaempferol					
Observed	Qi[a]	Scaled	Pot. energy distrib[b,c]		
399 sh	Q76	399 vw	88 **C**COop	21 tCCf	13 **C**q16a
376 w	Q77	374 w	105 t**A**CO7		
–	Q54	369 vw	38 **C**COip	33 **C**═**O**ip	
360 vw	Q78	362 w	103 t**B**CO		
–	Q55	340 vw	35 **A**CO7ip	15 **A**CO5ip	13 **C**q6a
–	Q79	317 vw	37 **C**q16b	36 **C**q4	22 **B**q4
–	Q56	300 vw	29 **C**COip	24 **B**CCir	21 **C**CCir
–	Q80	277 vw	183 tCCf	58 **A**q16b	31 **C**q16b
–	Q57	244 vw	13 **C**q6a	11 **B**CCir	
–	Q81	238 vw	56 **A**q16b	43 **A**q16a	20 **C**q16a
–	Q58	235 vw	12 **B**q6a	12 **C**Cir	
–	Q82	218 vw	53 **A**q4	25 **A**CHop	22 tCCf
–	Q83	144 vw	46 **C**q4	29 **C**q16a	21 **B**q16a
–	Q84	109 vw	61 **C**q16b	34 **B**q16a	
–	Q59	94 vw	35 **C**CCir	19 **B**CCir	
–	Q85	80 vw	110 **C**q16a	65 tCCf	28 **A**q16b
–	Q86	41 vw	46 **C**q16b	20 **C**COop	20 **C**q4
–	Q87	24 vw	111 tCCir		

[a] Q1–Q59 in-plane modes, Q60–Q87 out-of-plane modes.
[b] The first letter designates the ring: **A**-, **C**-, and **B**-ring; CC, CH, CO, OH—stretchings; **C**CCd—CC double bond stretching in **C**-ring; CCf—CC bond common to **A** and **C** rings; CHip(op)—CH in(out)-of-plane bendings; q12, q6a, q6b—linear combinations of CCC bendings (rings **A** and **B**) or CCC, CCO and COC bendings (ring **C**); q4, q12a, q12b—linear combinations of C(CC)C torsions (rings **A** and B) or C(CC)C, C(CC)O and C(CO)C torsions (ring **C**) (Table S3).
[c] OH3—OH stretching in C3—OH, COH3—COH bending in C3—OH etc.

C5—OH bendings, respectively. The assignment for the relatively strong bands at 1254 and 1225 cm^{-1} remains unclear, although they should be due to stretchings of C-ring and C5—OH bending, mainly.

The five strongest quercetin bands are two doublets at 1655 and 1649 cm^{-1} and another one at 1622 and 1616 cm^{-1}, followed by bands at 1514, 1317 and 1163 cm^{-1}. The doublets are most likely due to the factor group splitting (quercetin monohydrate has four [10], while quercetin dihydrate two molecules per unit cell [9]). The first doublet is related to the CC stretchings of A-ring, the second to the C2═C3 stretching of C-ring. The band at 1560 cm^{-1} is assigned to the C═O stretching and this presents a shift of 100 cm^{-1} with respect to flavone. Here again the C═O stretching is found below the bands to which the C2═C3 double bond stretching in C-ring contributes. Putting it differently, the force constant *f*C═O in quercetin (0.993 kN m^{-1}) is smaller than in flavone (1.170 kN m^{-1}) (Table 5). Three strong bands at 1514, 1317 and 1163 cm^{-1} correspond to the CC stretchings of A-ring, C3—OH bending of C-ring or C3′—OH bending of B-ring and C4′—OH bending of B-ring, respectively. The strong coupling between C═O and C2═C3 stretchings is understandable in terms of the force constant values which are 1.060 ± 0.070 kN m^{-1} and 0.846 ± 0.023 kN m^{-1}, respectively (Table 5).

In myricetin IR spectrum the five strongest bands are found at 1664, 1595, 1520, 1327 and 1030 cm^{-1}. The first and the third are due to the CC stretchings of A-ring. The second one can be attributed to the C═O stretching. The bands at 1327 (the strongest band in the spectrum) and 1030 cm^{-1} are contributed mainly by C3′—OH bending and C5′—O stretching, respectively.

The region 1800–1000 cm^{-1} in myricetin is most poorly reproduced. For example, the strong transition calculated at 1275 cm^{-1} (C4—O stretching and C3—OH bending) has no counterpart in the observed spectrum. In pyrogallol the C4′—O stretching is assigned to the observed band at 1258 cm^{-1} (calculated at 1259 cm^{-1}) (Table S20). Therefore, most likely myricetin molecules in crystal take part in hydrogen bonding among themselves and probably water molecules. This has been recently confirmed by Muresan-Pop et al. [16]. Myricetin monohydrate reveal a structure of an infinite 2D network of hydrogen-bonded molecules with water molecules positioned in between the infinite chains. Similar situation is documented for pyrogallol that is water-soluble solid. The spectra of pyrogallol anhydrate and hydrate are obviously different, particularly in the 1400–1200 cm^{-1}region where the bands due to CO stretchings and COH bendings are present (Table S20) [32].

3.2. Hydroxyl Groups

3.2.1. Hydroxyl OH Stretching

The OH stretchings are the most informative concerning the interactions with the surroundings, but their analysis is far from simple and most often deemed impossible. They appear as a strong, very broad and unstructured band covering the region 3700–3000 cm^{-1}. It is not possible to reproduce it within the harmonic approximation of a single molecule, although the present calculations give estimates of wavenumber shifts due to the hydrogen bond formation. Not only OH stretching, but all other OH group vibrations are affected by hydrogen bonding. Intermolecular hydrogen bonds are quite common in solid phases of flavonoids and this has to be taken into account when comparing a spectrum calculated for single molecule and the spectrum of a crystalline phase.

The (C7—) OH stretching band is predicted at 3626 ± 1 cm^{-1} for galangin (Table S11), kaempferol, quercetin and myricetin which is equal to the OH stretching in 7-chromone calculated at 3627 cm^{-1} It is not far from the observed OH stretching bands in the gas phase 6-hydroxyflavone (3650 cm^{-1} [19]) and phenol (3655 cm^{-1} [33,34, 35]). The observed OH bands of solid kaempferol, quercetin and myricetin show that the (C7—) OH groups are involved in intermolecular hydrogen bonding. In kaempferol and apigenin (Table S13) the only OH stretching of B ring is calculated at 3624 cm^{-1} which is by only 7 cm^{-1} lower than in phenol. In catechol the two OH bands are at 3663 (calculated at 3647 cm^{-1}) cm^{-1} and 3605 (3595) cm^{-1} (Table S15). For quercetin only the calculated values 3640 and 3598 cm^{-1} are available as are for myricetin (3642, 3598 and 3594 cm^{-1}). The myricetin values show slight variations in comparison to those of pyrogallol (3646, 3608 and 3591 cm^{-1}) (Table S20). Internally hydrogen bonded OH stretchings in flavones and flavonols are naturally predicted at much lower wavenumbers. In group **F** compounds the OH stretching at position 3 is predicted at 3382 cm^{-1} in 3-hydroxyflavone (measured at 3386 cm^{-1} in the gas phase) (Table S8) and at 3375 cm^{-1} in fisetin (Table S16). In group **A** molecules the OH stretching at position 5 of 5-hydroxyflavone is calculated at 3103 cm^{-1} (Table S9). This is approximately 50 cm^{-1} higher than in chrysin (3042 cm^{-1}) (Table S10), apigenin (3061 cm^{-1}) (Table S13) and luteolin (3037 cm^{-1}) (Table S17). In group **Q** (galangin (Table S11), kaempferol (Table S14), quercetin (Table S18), morin (Table S19) and myricetin (Table S21)) there are two intramolecular

Table 3
Observed IR and Raman and scaled wavenumbers of quercetin.

Quercetin								
IR	IR[a]	Raman[a]	Qi[b]	Si[b]	Scaled	Pot. energy distrib.[a]		
–	–	–	Q1	S1	3640 w	100 BOH4		
–	–	–	Q2	S2	3627 w	100 **AOH7**		
–	–	–	Q3	S3	3598 w	100 BOH3		
3388 vs bd	–	–	Q4	S4	3426 m	99 **C**OH		
	3368	3355						
		3321						
3290 sh	3290	3250	Q5	S5	3188 s	98 **AOH5**		
–	–	–	Q6	S6	3125 vw	99 **B**CH		
–	–	–	Q7	S8	3101 vw	100 **B**CH		
–	3093	3089	Q8	S7	3098 vw	99 **A**CH		
–	–	–	Q9	S9	3061 vw	100 **A**CH		
–	–	–	Q10	S10	3039 vw	99 **B**CH		
2960 w	–	–			–			
2923 w	–	–			–			
2852 w	–	–			–			
	1670							
1674 sh	1662				–			
1655 s		1657	Q11	S11	1655 vs	25 **A**CC	15 **A**CC	
1649								
1622 s			Q12	S12	1633 w	33 **C**CCd	13 **B**CC	
1616 s	1615	1620	Q13	S13	1621 m	20 **B**CC	18 **C**CCd	12 **B**CC
–		1613			–			
–			Q14	S**14**	1604 m	26 **C═O**	13 **A**CC	
1599 sh		1589	Q15	S15	1599 s	23 **B**CC	13 **B**CC	
1560 m	1559	1557	Q16	S**16**	1571 w	32 **C═O**	16 **A**CC	13 **A**CC
–		1549			–			
1522 sh	1520		Q17	S17	1521 w	19 **B**CHip	16 **B**CC	11 **B**CHip
1514 s	1512	1514	Q18	S18	1507 vs	15 **A**CC	14 **A**CHip	11 **A**CC
	1503	1500						
1479 w sh	–	–	Q19	S19	1485 m	22 **ACOH5**	13 **C**CC	11 **C═O**
–	1458	1463	Q20	S20	1463 vw	17 **B**CC	15 **B**CHip	15 **B**CC
–	1431	1435			–			
–	–	–	Q21	S21	1438 w	18 **C**CC	12 **ACO5**	
1431 m	–	–			–			
–	–	1399	Q22	S22	1407 vw	28 CCf	23 **ACOH5**	21 **A**CC
–	–		Q23	S23	1383 m	14 **C**COH	14 **ACO5**	13 **A**q12
1369 s	–	1371			–			
	1362							
1350 sh	1353		Q24	S24	1356 vw	23 **B**CC	21 **B**CC	18 **B**CC
–	–	–	Q25	S25	1340 vw	30 **A**CC	15 **A**CC	13 **C**CC
–		1328	Q26	S26	1331 s	31 **C**COH	26 CCir	11 **B**CHip
1317 s	1316	1316	Q27	S27	1316 s	27 **BCOH3**	18 **B**CHip	
–	–	–	Q28	S28	1293 w	19 **BCO4**	15 **B**CHip	15 **B**CC
1288 w	1288	1288			–			
–	–	–	Q29	S29	1272 s	11 **A**CC	11 **ACOH5**	
–	–	–			–			
1244 s	1244	1239	Q30	S30	1243 vw	29 **ACOH7**	18 COr	
–			Q31	S31	1239 vw	21 **BCO3**	14 **C**CO	
1207 s	1211	1208	Q32	S32	1206 m	26 COr	11 **C**CO	
–	–	–	Q33	S33	1197 m	28 **BCOH3**	18 **B**CHip	11 **B**CC
–	–	–	Q34	S34	1179 vw	29 **A**CHip	13 **ACO7**	11 **ACOH7**
1163 s	1164	1158	Q35	S35	1159 vw	25 **BCOH4**	21 **B**CHip	
–	–	–	Q36	S36	1158 s	27 **A**CHip	26 **ACOH7**	12 **ACO7**
	1143							
–		1135	Q37	S37	1123 m	13 COr	11 **BCOH4**	
–	1102	1103	Q38	S38	1110 w	19 **BCOH4**		
1092 s	1093	1092	Q39	S39	1093 vw	26 COr		
1015 m			Q40	S40	1017 vw			
1009 m	1010	1007			–			
999 m	999	998	Q41	S41	998 vw	13 **A**q12	12 **A**CC	
–			Q42	S42	940 vw	12 **A**q12	12 **C═O**ip	12 **B**q12
931 m	932	930	Q43	S62	935 vw	81 **B**CHop	42 **B**CHop	
883 w	883	885	Q44	S63	885 vw	121 **B**CHop	19 **B**q4	
	861							
	847	845						
841 w	842		Q45	S43	838 vw	26 **B**q12	21 **C**q12	
–		–	Q46	S64	825 vw	57 **A**CHop	52 t**ACO5**	
818 w	818	–	Q47	S65	813 vw	111 **A**CHop	15 **A**q16b	11 **A**q4
808 w	808	–	Q48	S66	807 vw	76 **B**CHop	33 **B**CHop	11 **B**COop
–	793	792	Q49	S67	804 w	61 **A**CHop	40 t**ACO5**	24 **A**q4
788 w	787	–	Q50	S44	791 vw	24 **B**CC	16 **BCO4**	
–	–	–	Q51	S68	720 vw	113 **C═O**op	84 **C**q4	75 tCCf

(continued on next page)

Table 3 (*continued*)

Quercetin								
IR	IR[a]	Raman[a]	Qi[b]	Si[b]	Scaled	Pot. energy distrib.[a]		
–	–	–	Q52	S45	713 vw	22 **C**q12		
703 w	–	–	Q53	S69	699 vw	152 **B**q4	41 **B**COop	33 **BCO3**o
689 vw	–	–			–			
–	–	–	Q54	S46	684 vw	16 **A**q12		
–	–	–	Q55	S70	678 vw	73 **A**q4	40 **ACO5**op	28 tCCf
–	–	–	Q56	S71	657 vw	43 **A**q4	25 **BCO3**op	24 ir**C**CC
638 w	638	641	Q57	S47	639 vw	16 **A**q6b	12 CCf	11 **C**═**O**ip
–	–	–	Q58	S72	633 vw	104 **ACO7**op	47 **A**q16b	26 **A**q4
609 vw	–	–	Q59	S73	611 w	84 tCCO	14 **C**q4	
–	–	–	Q60	S74	605 vw	41 **ACO5**op	38 **C**q4	33 **A**q16a
–	–	–	Q61	S48	604 vw	28 **B**q6b		
598 w	598	598			–			
–	–	–	Q62	S49	588 vw	14 **BCO4**ip	13 **BCO3**ip	
–	–	–	Q63	S50	576 vw	18 **A**q6a	13 **B**q6b	
569 vw	564	567			–			
551 vw	–	–			–			
–	–	–	Q64	S75	544 vw	33 ir**C**CC	32 **B**q4	25 **C**q16b
–					–			
521 vw	519	522	Q65	S51	523 vw	28 **A**q6a	25 **C**q6b	25 **A**q6b
–		517			–			
494 vw	495	490			–			
–			Q66	S52	482 vw	18 **B**q6b	14 **C**q6a	13 **BCO3**ip
461 vw	465	460			–			
–			Q67	S53	456 vw	18 **C**q6b	16 **B**q6a	11 **A**q6a
–	443	447	Q68	S76	450 vw	80 **B**q16b	46 **BCO3**op	36 **B**COop
410 vw-			Q69	S77	419 w	92 t**BCO3**	12 **B**COop	
–			Q70	S78	401 vw	24 **A**q6b	16 **ACO5**i	15 **C**q6a
–			Q71	S54	401 vw	84 **C**COop	19 tCCf	13 **C**q16a
–			Q72	S79	374 w	105 t**ACO7**		
370 vw			Q73	S55	370 vw	40 **C**COip	35 **C**═**O**ip	
–			Q74	S56	339 vw	37 **ACO7**i	15 **ACO5**i	13 **C**q6a
–			Q75	S80	339 vw	26 **C**q4	25 **B**COop	21 **B**q16b
–			Q76	S57	310 vw	46 **BCO4**i	33 **BCO3**i	
–			Q77	S58	287 vw	22 **C**COip	21 **C**CCip	16 ir**B**CC
–			Q78	S81	280 vw	177 tCCf	47 **C**q16b	44 **A**q16b
–			Q79	S82	256 w	70 t**BCO4**	18 **A**q16b	18 **C**q4
–			Q80	S83	245 vw	36 **A**q16b	35 t**BCO4**	21 **C**q4
–			Q81	S59	236 vw	15 ir**B**CC		
–			Q82	S60	228 vw			
–			Q83	S84	224 vw	33 **A**q16a	31 **A**q4	25 **A**CHop
–			Q84	S85	204 vw	28 **B**q16b	20 **B**q4	18 **B**q16a
–			Q85	S86	143 vw	44 **C**q4	27 **C**q16a	26 **B**q16a
–			Q86	S87	110 vw	59 **C**q16b	36 **B**q16a	
–			Q87	S61	85 vw	32 **C**CCip	23 ir**B**CC	
–			Q88	S88	80 vw	109 **C**q16a	66 tCCf	28 **A**q16b
–			Q89	S89	40 vw	46 **C**q16b	20 **C**COop	20 **C**q4
–			Q90	S90	13 vw	124 tCCir	17 **C**COop	

[a] [13].
[b] Qi—the i-th normal mode when they are ordered in descending order of their wavenumbers. Si—the i-th normal mode when they are ordered within the symmetry classes: A′ (in-plane modes) S1–S61, A″ (out-of-plane modes) S62–S90.

hydrogen bonds. The stronger one (C5—OH···O═C) is at 3424 ± 6 cm^{-1} while the weaker one (C3—OH···O═C) at 3094 ± 14 cm^{-1}.

3.2.2. Hydroxyl CO Stretching

A phenol molecule with a single OH group may be taken as an unperturbed system when compared to catechol, pyrogallol and other flavonols. In phenol the hydroxyl CO stretching is calculated at 1262 cm^{-1} (Table S12). In catechol with two neighboring OH groups two modes are predicted at 1283 and 1246 cm^{-1} (Table S15) and in pyrogallol only two modes, at 1259 and 997 cm^{-1}, are pure CO stretching modes (Table S20). In 7-hydroxychromone the hydroxyl group is attached to a different ring system and its CO stretching is found at 1282 cm^{-1}, i.e. 20 cm^{-1} higher than in phenol (Table S5). Hydroxyl CO stretchings are thus within 1800–1000 cm^{-1} region giving rise to some of the strongest bands in that region. In flavonoids they are found in the same spectral region. An explanation for such a frequency spread can be formulated by means of the values of the stretching force constants, *f*CC and *f*CO, of the coupled internal oscillators. The *f*CC values are within 0.69–0.73 kN m^{-1} while those of *f*CO are within 0.62–0.72 kN m^{-1}. With comparable masses of the involved atoms, the extensive coupling occurs.

3.2.3. Hydroxyl In-plane COip and Out-of-plane Bending COop

It is observed that in phenol, catechol and pyrogallol the out-of-plane CO bendings are at higher wavenumbers than the in-plane bendings, 662 vs. 402 cm^{-1} in phenol, 689–455 vs. 553–308 cm^{-1} in catechol. In apigenin (Table S13) and kaempferol (Table 2) the COop and COip bending vibrations of the B ring significantly contribute to the normal modes at (726 and 514) cm^{-1} and at (437 and 410) cm^{-1}, respectively. In pyrogallol there are three CO bonds, but nevertheless the corresponding interval are close to those of catechol. The pyrogallol bands at 582 and 303 cm^{-1} are dominated by COip bending, while those at 311 and 295 cm^{-1} by COop bending. In myricetin the COip modes are located in the narrow interval 338–295 cm^{-1}. The COop bending modes are found at 571 and 347 cm^{-1}.

Table 4
Observed and calculated wavenumbers (scaled by $\nu_{i,scaled} = \nu_{i,calc} * (1 - 0.00001356 * \nu_{i,calc})$) of myricetin.

Myricetin							
IR	IR[a]	Raman[a]	Qi[b]	Scaled	Pot. energy distrib.		
–	–	–	Q1	3642 vw	100 **BOH5**		
–	–	–	Q2	3626 w	100 **AOH7**		
–	–	–	Q3	3598 w	97 **BOH4**		
–	–	–	Q4	3594 w	97 **BOH3**		
3494 sh	–	–		–			
–	–	–	Q5	3418 w	99 **C**OH		
3414 vs	3408 vs	–		–			
3352 vs	–	–		–			
–	3341 vs	–		–			
3294 vs	3296 vs	–		–			
–	–	–	Q6	3194 s	98 **AOH5**		
3107 sh	–	–	Q7	3109 vw	100 **B**CH		
–	–	–	Q8	3099 vw	99 **A**CH		
–	–	–	Q9	3098 vw	100 **B**CH		
–	–	–	Q10	3060 vw	100 **A**CH		
2957 w	2958 vw	–		–			
2926 w	2922 w	–		–			
2853 w	2852 w	–		–			
–	2714 vw	–		–			
–	2660 vw	–		–			
1662 vs	1662 s	1658 w	Q11	1655 s	25 **A**CC	16 **A**CC	
1654 sh	–	–			–	–	–
1649 w	–	–		–			
1631 m	1631 m	–	Q12	1633 w	27 **C**CCd	15 **B**CC	
1619 m	1618 m	1620 vs	Q13	1627 w	25 **B**CC	15 **B**CC	12 **B**CC
1606 m	1606 m	1609 s	Q14	1612 vw	22 **B**CC	17 **C**CCd	12 **B**CC
1595 s	1595 s	1596 sh	Q15	1603 vs	25 **C═O**	20 **A**CC	13 CCf
–	–	–	Q16	1570 vw	32 **C═O**	16 **A**CC	13 **A**CC
1555 m	1554 m	–		–			
1537 sh	–	1546 w	Q17	1537 m	14 **B**CC	12 **B**CHip	12 **B**CC
1520 vs	1521 vs	1516 w		1507 s	16 **A**CC	14 **A**CHip	11 **C**CC
1508 sh	–	–	Q18	1485 m	21 **ACOH5**	11 **C**CC	
1481 m	1483 w	–	Q19	–			
1466 m	1464 m	–	Q20	1468 vw	22 **B**CC	20 **B**CC	
1446 m	1446 m	–		–			
–	1436 m	1439 s	Q21	1437 w	18 **C**CC	12 **ACO7**	
–	–	–	Q22	1406 vw	28 CCf	23 **ACOH5**	21 **A**CC
1392 m	1391 m	–	Q23	1386 m	12 **B**CC	12 **ACO7**	12 **A**q12
1377 s	1377 s	1385 m	Q24	1382 m	17 CCir	17 **B**CC	15 **BCO5**
–	–	–	Q25	1360 vw	27 **B**CC	15 **B**CC	11 **B**CC
–	–	–	Q26	1338 w	30 **A**CC	13 **A**CC	13 **C**CC
1327 vs	1328 vs	1332 vs	Q27	1320 m	25 **BCOH3**	13 **B**CHip	
1300 s sh	1309 s	–		–			
–	–	–	Q28	1305 vw	24 **B**CHip	21 **C**COH	11 **BCOH5**
–	–	1266 w	Q29	1275 vs	17 **BCO4**	12 **C**COH	
–	1253 vw	–	Q30	1249 vw	13 **C**CO	11 **BCO4**	
–	1247 vw	–	Q31	1242 vw	28 **ACOH7**	18 **C**COr	11 **A**CHip
1228 s	1230 s	1230 w 1218 sh	Q32	1233 w	22 **BCOH4**	20 **BCO3**	20 **B**CHip
1203 s	1201 s	–	Q33	1200 s	30 **C**COr	16 **A**CHip	13 **C**CO
–	–	–	Q34	1192 vw	38 **BCOH3**	16 **B**CHip	16 **B**CC
1186 s	1186 m	–		–			
1168 s	1170 s	1171 w	Q35	1175 vw	24 **A**CHip	16 **ACOH7**	
–	–	–	Q36	1158 m	28 **A**CHip	26 **ACOH7**	12 **ACO5**
–	–	–	Q37	1152 w	47 **BCOH5**	18 **BCOH4**	
1108 m	1109 m	1116 w	Q38	1117 vw			
1090 m	1090 m	–	Q39	1097 vw	31 **C**COr		
–	–	–	Q40	1034 vw	15 **BCO3**	11 **BCO5**	
1030 s	1029 s	1030w	Q41	1026 m	18 **BCO5**		
1004 m	1005 m	–	Q42	1007 vw	18 **A**CC	16 **A**CC	11 **A**q12
939 w	939 w	939 w	Q43	939 vw	14 **A**q12	13 **C═O**ip	
864 vw sh	–	–	Q64	860 vw	123 **B**CHop		
855 w	855 m	–		–			
–	–	–	Q65	842 vw	123 **B**CHop	16 **B**q4	
829 w	831 m	833 w	Q44	831 vw	26 **B**q12	16 Cq12	12 **BCO4**
–	–	–	Q66	823 vw	72 **A**CHop	37 t**ACO5**	
–	–	–	Q67	813 vw	113 **A**CHop	16 **A**q4	15 **A**q12b
800 vw	–	–	Q68	802 w	56 t**ACO5**	48 **A**CHop	19 **A**q4
787 vw	788 m	–		–			
769 w	770 m	–	Q45	763 vw	14 **BCO4**	13 **C**q12	
729 w sh	730 m	–		–			
720 w	721 m	–	Q46	719 vw	20 **C**q12	11 **C**CCir	

(continued on next page)

Table 4 (*continued*)

Myricetin							
IR	IR[a]	Raman[a]	Qi[b]	Scaled	Pot. energy distrib.		
705 w	707 m	–	Q69	719 vw	113 **C═O**op	81 **C**q4	77 tCCir
–	–	–	Q70	686 vw	40 **C**CCir	38 **A**q4	32 **B**CCir
–	–	–	Q71	679 vw	168 **B**q4	89 **BCO4**o	63 **BCO3**o
–	669 vw	–	Q72	663 vw	81 **A**q4	32 **ACO5**o	23 **B**CCir
644 w	644 m	649 w	Q47	645 vw	12 **A**q6b		
–	–	–	Q48	641 vw	18 **C**q6a	14 **A**q12	
–	–	–		–	105 **ACO7**o	48 **A**q12b	25 **A**q4
623 vw	623 w	628 w	Q73	633 vw			
–	–	–	Q49	618 vw	13 **BCO4**i	12 **B**q6b	
610 vw	–	–	Q74	610 vw	90 tCCO		
–	–	–	Q75	604 vw	45 **C**q4	41 **ACO5**o	35 **A**q12a
–	–	–	Q50	577 vw	25 **A**q6a	12 **C**q6b	
575 w	575 w	576 w		–			
–	–	–	Q76	571 vw	75 **BCO5**o	65 **BCO3**o	65 **B**q16b
535 vw	537 w	534 w		–			
–	–	–	Q77	531 vw	40 **B**q16a	35 **B**q4	34 **C**CCir
–	–	–	Q51	530 vw	28 **B**q6b	11 **C**q6b	
–	–	–	Q52	527 vw	23 **B**q6a		
522 vw	521 w	520 w		–			
–	–	–	Q53	518 vw	28 **A**q6a	17 **A**q6b	14 **C**q6b
499 vw	505 w	–		–			
–	469 vw	–	Q54	459 vw	21 **C**q6b	12 **C**q6a	
–	–	–	Q78	431 vw	75 t**BCO3**	19 t**BCO4**	
417 vw	–	–		–			
406 vw	411 vw	–	Q55	401 vw	24 **A**q6b	15 **ACO5**i	15 **C**q6a
–	–	–	Q79	399 vw	82 **C**COop	19 tCCir	13 **C**q16a
–	–	–	Q80	376 m	77 t**ACO7**	20 t**BCO4**	
–	–	–	Q81	374 vw	57 t**BCO4**	28 t**ACO7**	21 t**BCO3**
–	–	–	Q56	371 vw	42 **C**COip	34 **C═O**ip	
349 w	–	–	Q82	347 vw	52 **BCO4**op	28 **BCO5**op	17 **C**q4
332 vw sh	–	–	Q57	338 vw	38 **ACO7**ip	17 **ACO5**ip	12 **C**q6a
–	–	–	Q58	317 vw	33 **BCO5**ip	32 **BCO3**ip	19 **B**q6a
–	–	–	Q59	295 vw	62 **BCO4**ip	16 **BCO5**ip	12 **B**q6b
–	–	–	Q60	284 vw	21 **C**CCir	20 **C**COip	12 **B**CCir
–	–	–	Q83	280 vw	180 tCCir	48 **C**q16b	44 **A**q12b
–	–	–	Q84	254 vw	36 **B**q16b	25 **C**q4	25 **A**q12b
–	–	–	Q85	250 vw	82 **B**q16b	17 t**BCO5**	15 **A**q12b
–	–	–	Q86	239 w	70 t**BCO5**	18 **A**q12b	13 **A**q12a
–	–	–	Q61	228 vw	17 **B**CCir		
–	–	–	Q87	222 vw	42 **A**q4	27 **A**CHop	26 **A**q12a
–	–	–	Q62	211 vw	11 CCir		
–	–	–	Q88	175 vw	40 **B**q4	17 **B**q16a	17 **C**q16a
–	–	–	Q89	140 vw	43 **B**q16a	36 **C**q4	20 **C**q16a
–	–	–	Q90	110 vw	57 **C**q16b	41 **B**q16a	
–	–	–	Q63	83 vw	31 **C**CCir	25 **B**CCir	
–	–	–	Q91	81 vw	108 **C**q16a	65 tCCir	28 **A**q12b
–	–	–	Q92	39 vw	45 **C**q16b	22 **C**COop	22 **C**q4
–	–	–	Q93	15 vw	110 tCCir		

[a] [23].
[b] Q1–Q63 in-plane modes, Q64–Q93 out-of-plane modes.

3.2.4. Hydroxyl COH Bending

In phenol the COH bending is at 1173 cm^{-1}, in catechol they are at 1181 and 1144 cm^{-1}. The pyrogallol COH bendings are situated at 1240, 1181 and 1142 cm^{-1}. The wavenumber increase upon the hydrogen bonding formation is even greater in 3,5,7-trihydroxychromone. The leading C7—OH bending contributions are found at 1228 and 1163 cm^{-1}, for C3—OH at 1261 cm^{-1} and for C5—OH at 1482 and 1406 cm^{-1}. The bendings are thus above 1000 cm^{-1} and some of the strongest bands are to be attributed to the COH bending vibrations.

It is known that the presence of catechol moiety enhances the antioxidant activity of flavonoids by strongly affecting the C3—OH group [2]. It might be of interest to search for any spectroscopic evidence of presence of catechol-like bands in the interval 1800–1000 cm^{-1}. By examining the calculated spectra of fisetin, luteolin and quercetin (Fig. S6) it is not possible to find any band that could be characterized as catechol band. This will be confirmed also by mixing analysis (see below)! From the fact that the OH stretching in 3-hydroxyflavone is predicted at 3382 cm^{-1} and at 3375 cm^{-1} in fisetin, and that the COH bending is at 1327 cm^{-1} in 3-hydroxyflavone and at 1333 cm^{-1} in fisetin, one concludes that the influence of catechol on the C3—OH group is not essential.

3.2.5. Hydroxyl Torsion tCO

Torsions around CO bonds are below 500 cm^{-1} and therefore not normally accessible in the IR experiments with flavonoids in solution or solid phase. However, when a COH group is a part of the hydrogen bond the torsion occurs at much higher wavenumbers, for example, at 650 cm^{-1} in 3-hydroxyflavone, at around 870 cm^{-1} and 130 cm^{-1} in 5-hydroxyflavone, and in galangin at 826, 804 and 605 cm^{-1}.

3.3. Carbonyl Group and Its Surrounding

3.3.1. Carbonyl Stretching C═O

Most often the strongest band within 1600 ± 100 cm^{-1} was attributed to the C═O stretching vibration, but it has been recognized that it need not be the case [13,23,36]. In order to reveal the details of the related frequency shifting and intensity redistribution three chromones with no substituents at positions 3 and 5 were also studied, namely,

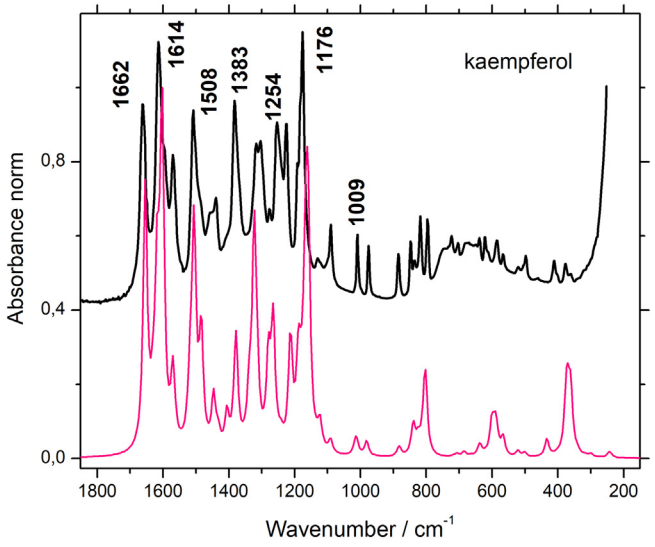

Fig. 2. Observed (black) and calculated (red) IR spectra of kaempferol. (For interpretation of the references to color in this figure legend, the reader is referred to the web version of this article.)

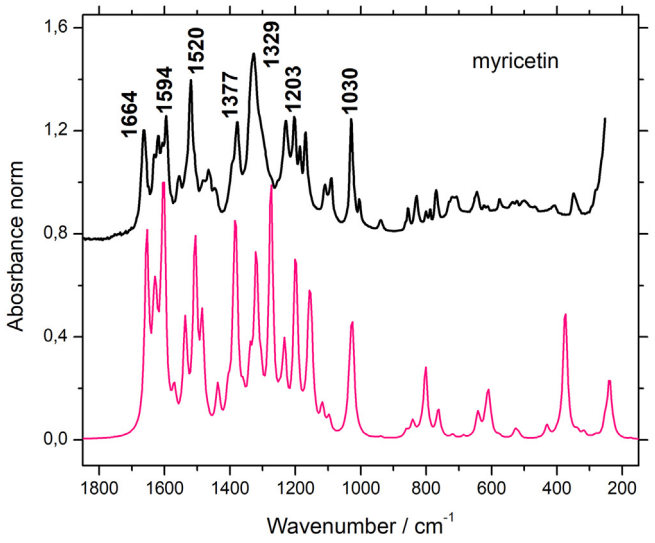

Fig. 4. Observed (black) and calculated (red) IR spectra of myricetin. (For interpretation of the references to color in this figure legend, the reader is referred to the web version of this article.)

chromone itself (Table S4), 7-hydroxychromone (Table S5) and 3,5,7-trihydroxychromone(Table S6).

In flavone (Table S7) the calculated value of 1673 cm^{-1} agrees well with the value of 1683 cm^{-1} measured in gas phase [19] and this band can obviously be assigned to the C═O stretching. In solid phase, the bands at 1646 and 1636 cm^{-1} observed in IR and Raman spectrum, respectively, should also be interpreted as due to the C═O stretching. The difference of 10 cm^{-1} of the latter two, i.e. the non-coincidence of the IR and Raman values, is caused by the factor group splitting while the lowering of 40–50 cm^{-1} relative to the gas phase is manifestation of the intermolecular interactions in the crystal (space group symmetry of flavone crystal is $P2_12_12_1$ with Z = 8 molecules in the unit cell with two molecules per asymmetric unit. The chromone part makes a dihedral angle of 1.0 (1)° with the 2-phenyl substituent in one of them, while in the other the chromone part makes a dihedral angle of 9.8 (1)° with the 2-phenyl substituent [14]).

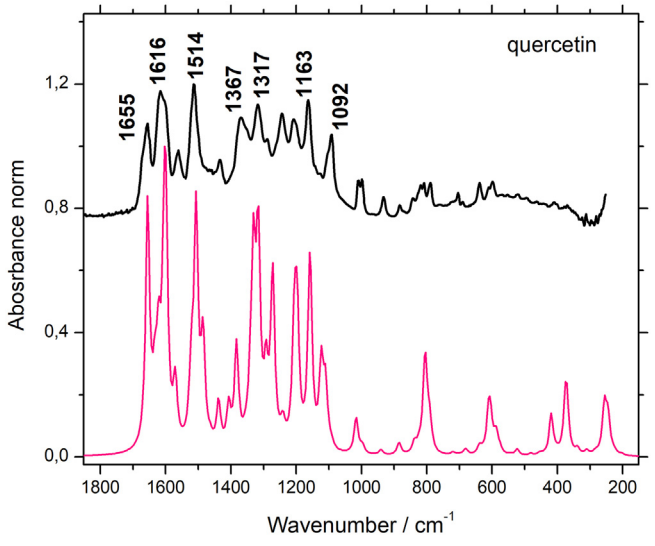

Fig. 3. Observed (black) and calculated (red) IR spectra of quercetin. The shoulders of the 1655 and 1616 cm^{-1} bands of quercetin are quite clearly seen and their precise wavenumbers were determined by taking the second derivative of the spectrum (Table 3). The same resolution enhancement was applied also to kaempferol and myricetin spectra. (For interpretation of the references to color in this figure legend, the reader is referred to the web version of this article.)

The next step would be to reveal the effects of hydroxyl substitution on positions 3 and 5. In both cases an intramolecular hydrogen bond is formed and it is known that the one in 5-hydroxyflavone is stronger than in 3-hydroxyflavone. Geometrically this is obvious from the departure of the angle O—H···O from 180° which is 31° in 5-hydroxyflavone and 60° in 3-hydroxyflavone. In kaempferol as in other group **Q** flavonoids (Table 1) the C═O stretching contributes to two bands at around 1600 and 1570 cm^{-1} (Table 2) which is a shift of about 70 cm^{-1} in comparison to flavone. The normal modes will accordingly be very much mixed in character and only approximate correspondence between the normal modes of the two molecules with those of unsubstituted chromone will be possible (Tables 2, 3, and 4). This can be seen on two ways, through the potential energy distribution, i.e. values of *f*C═O and *f*C2═C3 stretching constants (Table 5) and through and the mixing coefficients (Table 6) (see further on). Phenyl substituent induces the lowering of the *f*C2═C3 force constant from 0.894 (chromone and 7-hydroxylchromone) to 0.839 kN m^{-1} (flavone). At the same time the largest *f*C═O stretching constant is calculated for 7-hydroxychromone (1.178 kN m^{-1}), followed by flavone (1.170 kN m^{-1}) and chromone (1.168 kN m^{-1}). There is a clear trend in the values *f*C═O that follows the substitution pattern at the positions 3 and 5. The mean values for the respective groups are: 1.178 ±

Table 5
Force constants for C═O and C2═C3 stretchings.

Group	Name	Planar	*f*C═O[a]	*f*C2═C3[a]
C	Chromone	Yes	1.186	0.892
	7-Hydroxychromone	Yes	1.178	0.896
	Flavone	No	1.170	0.839
F	3-Hydroxyflavone	Yes	1.107	0.828
	Fisetin	Yes	1.096	0.834
A	5-Hydroxyflavone	No	1.051	0.836
	Chrysin	No	1.039	0.841
	Apigenin	No	1.039	0.836
	Luteolin	No	1.035	0.835
Q	3,5,7-Trihydroxychromone	Yes	1.023	0.878
	Galangin	Yes	1.000	0.832
	Kaempeferol	Yes	0.993	0.828
	Morin	No[b]	0.998	0.855
	Quercetin	Yes	0.994	0.830
	Myricetin	Yes	0.993	0.830

[a] Force constants (kN m^{-1}) for C═O and C2═C3 double bond stretchings.
[b] If there **is** a hydrogen bond between OH at 2 and OH at 3′ morin is non-planar. If there is **no** such bond it is planar.

Table 6
Normal modes of selected flavones in terms of flavone normal modes.

			3-Hydroxy	flavone		
Qi	$\tilde{\nu}$	Rel. IR int.	$\Delta\tilde{\nu}$[a]	Mixing	Coeff.	
11	1645	m	27	0.59 Q11	0.47 Q12	0.46 Q13
12	1625	vs	−10	0.74 Q13	−0.64 Q11	
13	1619	s	5	−0.81 Q12	0.40 Q14	0.34 Q11
14	1611	w	2	−0.90 Q14		
15	1584	vw	5	−0.97 Q15		
16	1576	w	1	−0.92 Q16		
			5-Hydroxy	flavone		
Qi	$\tilde{\nu}$	Rel. IR int.	$\Delta\tilde{\nu}$[a]	Mixing	Coeff.	
11	1657	vs	−32	0.75 Q12	−0.53 Q11	
12	1618	s	−3	0.66 Q13	−0.63 Q11	−0.33 Q12
13	1613	m	1	−0.95 Q14		
14	1604	vw	11	0.65 Q13	0.50 Q12	0.37 Q15
15	1587	vw	2	−0.81 Q15	−0.38 Q16	
16	1580	vw	−3	−0.88 Q16	0.41 Q15	
			Kaempferol			
Qi	$\tilde{\nu}$	Rel. IR int.	$\Delta\tilde{\nu}$[a]	Mixing	Coeff.	
11	1654	s	−30	0.86 Q12		
12	1631	vw	−16	0.85 Q13		
13	1618	m	−5	−0.88 Q14		
14	1603	vs	69	0.65 Q11	0.57 Q16	
15	1588	vw	1	−0.89 Q15		
16	1570	w	7	−0.61 Q16	0.57 Q11	

[a] $\Delta\tilde{\nu}$—difference between the wavenumber of the leading flavone normal mode with the largest mixing coefficient and the corresponding normal mode wavenumber of a flavone derivative.

0.008 kN m^{-1} (group C), 1.102 ± 0.005 kN m^{-1} (group **F**), 1.041 ± 0.010 kN m^{-1} (group A) and 0.996 ± 0.004 kN m^{-1} (group **Q**).

3.3.2. Carbonyl In-plane (C═Oip) and Out-of-plane Bending (C═Oop)

In chromone the normal modes with contributions of the carbonyl in-plane bending C═Oip are calculated at 575, 529 and 287 cm^{-1}. Actually the latter is almost pure mode and thus it turns out that the carbonyl in-plane bending C═Oip in chromone is rather low. On the other hand, the pure C═Oip vibration in flavone is predicted only at 606 cm^{-1}. While it remains at nearly the same position at 617 cm^{-1} in 5-hydroxyflavone, it is significantly downshifted to 367 cm^{-1} in 3-hydroxyflavone. Contributions of the carbonyl out-of-plane bending C═Oop are calculated at higher wavenumbers 836, 751 and 672 cm^{-1} in chromone and at 854 and 678 cm^{-1} in flavone. Obviously, the presence/absence of hydroxyl groups at positions 3 and 5 greatly influences not only the C═O stretching vibration, but the other vibrations of the C═O group as well. Thus, to some extent only C═O stretching might be useful in understanding interactions of flavonoids with their surroundings.

3.4. Harmonic Mode Mixing Analysis

As has been already mentioned there are many ways to choose the reference molecule when doing the mixing analysis. The flavone molecule might be a good choice because all other flavonols can be derived from it by simply adding hydroxyl groups. This is quite analogous to the problem of phenol, catechol and pyrogallol which are benzene derivatives. As already mentioned all flavonoids lacking hydroxyl substitution at position 3 are slightly non-planar in their ground states. In order to enable the mixing analysis for all studied molecules, the optimized non-planar flavonoids were made planar by setting the dihedral angle ∠(C3, C2, C1′, C2′) to zero. Frequency calculations gave one imaginary frequency as a consequence of the structure instability against internal rotation about the inter-ring C2—C1′ bond. Other normal modes remain unaffected because the corresponding torsion is not significantly coupled to any other internal coordinate.

Having decided to use flavone as a reference molecule when interpreting the observed and calculated spectral patterns of other studied molecules in the range 1700–1500 cm^{-1}, the assignments for flavone deserve few words of comment. The flavone normal modes of interest for further discussion are Q11 (C═O stretching), Q12 (C2═C3 stretching and CC stretchings of A-ring), Q13 (C2═C3 stretching and CC stretchings of B-ring), Q14 (CC stretchings of B-ring), Q15 (CC stretching of B-ring) and Q16 (C2═C3 stretching and CC stretchings of A-ring) (Table S7).

In harmonic mode mixing analysis the degree of similarity between the atomic movements performed during the normal vibrations is measured. Usually the overall picture is consistent with the interpretation based on the potential energy distribution, but in some cases it is not. The reason is that only the first three most significant contributions in the potential energy distribution are shown and those can be due to the part of a molecule that is not considered in the mixing analysis. For example, the flavone mode Q14 corresponds to the mode Q9 of chromone although according to the potential energy distribution it is mainly the CC stretchings of B-ring that contribute (Table 6). Nevertheless, it can be safely concluded that the C═O stretching is lowered from around 1680 to around 1600 cm^{-1}. Its intensity is also changed and in 3,5-dihydroxyflavones it is no longer the dominant band in that region.

The sort of question that is best answered by the mixing analysis is the following. In flavone the normal mode Q11 at 1673 cm^{-1} is pure C═O stretching. What happens to this mode in a bigger molecule, i.e. in a hydroxyl derivative of flavone, for example 3-dihydroxyflavone, 5-dihydroxyflavone and kaempferol as typical examples of groups F, A and Q (Table 1)? The answer is found in Table 6. There is no more a mode that could be termed C═O stretching mode in any of the selected substituted flavones. It is clear that only through mixing of flavone modes Q11, Q12 and Q13 the highest modes of 3- and 5-hydroxyflavone can be properly described. At the same time, this mixing is absent in kaempferol where seems to be quite acceptable to say that in all group Q compounds the C═O stretching is lowered by 70 cm^{-1}.

The four strongest bands of gaseous catechol are observed at 1508, 1260, 1160 and 740 cm^{-1}. It is not straightforward to pick the corresponding bands in solutions or solid (Table S15). Concerning the calculated ones, because the observed bands at 1260 and 1160 cm^{-1} look like doublets, they are at 1515 (Q9), 1283 (Q13), 1246 (Q14), 1184 (Q15), 1144 (Q17) and 743 (Q25) cm^{-1}. The first one and the last one are due to CH in-plane and CH out-of-plane bendings, while the first doublet is assigned to CO stretchings and the second one to COH bendings (Table S15). With an idea to identify the vibrations of catechol and pyrogallol OH groups in the spectrum of a flavonol, i.e. to answer the question what are the modes Q13, Q14, Q15 and Q17 transformed in, the mixing analysis for quercetin and myricetin has been performed. The quercetin modes showing resemblance with these four catechol modes are Q28, Q29, Q31, Q33, Q35 and Q36 ranging from 1300 to 1150 cm^{-1} (Table S18). Unfortunately they are not the only modes in this interval. Quite analogously, the pyrogallol modes Q14, Q15, Q16, Q18 and Q20 can be found in myricetin normal modes occurring in the range 1270–1020 cm^{-1} (Table S21). At the same time it is observed that there are a number of quercetin (myricetin) modes that bear no resemblance to any of the catechol (pyrogallol) modes. This proves that the coupling between chromone and phenyl part of a flavone is generally weak. In other words, the coupling is realized only in some of the flavone normal modes.

4. Conclusions

In spite of structural similarities in the chromone part the band assignments for kaempferol, quercetin and myricetin in the interval 1700–1500 cm^{-1} differ because most of the B ring modes that are

dependent on its substitution pattern fall in this region. The analysis also revealed that any flavone or flavonole molecule can be considered as composed of two weakly coupled parts with characteristic vibrations of each part spread over the whole interval 1800–100 cm^{-1}. In addition, since the intensities of IR transitions are proportional to the derivatives of the molecular dipole moment over normal coordinates, an extensive redistribution of vibrational intensities takes place. That is why the spectra of structurally not so different molecules bear relatively little resemblance. An additional complication is that any structural change caused by interactions with molecular environment (conformational change, deprotonation, …) cannot stay localized in a narrow part of the spectrum, but affects practically the whole spectrum.

Therefore, it can hardly be satisfactorily to discuss the spectra of flavonoids in terms of characteristic vibrations of either hydroxyl or carbonyl group. Only the simplest cases of phenol and catechol are tractable that way. Very often the strongest band around 1600 cm^{-1} was attributed to the C═O stretching vibration, but that is not the case as has been clearly shown. The reason lies in the quite comparable values of, for example, CO stretching and CO bending force constants and stretching and deformation force constants of rings giving rise to an extensive coupling (mixing) between internal oscillators.

The antioxidant activity (ability to reduce DPPH (2,2-diphenyl-1-picrylhydrazyl) into DPPH-H) was found to decrease according to the order quercetin > luteolin > kaempferol > galangin [37]. The former two, unlike the latter two, possess catechol type ring. In the present analysis it has turned out that the coupling of internal oscillators of the adjacent hydroxyl groups enhanced by intramolecular hydrogen bond is certainly equally important as the mere presence of the hydroxyl groups. This sort of coupling results in higher reactivities of hydroxyl groups towards hydrogen and electron donation to the various radicals.

An interesting observation also made in earlier studies is that all observed IR transitions below 1000 cm^{-1} are of much lower intensity. Thus, the bands in the region above 1000 cm^{-1} dominate IR spectra of kaempferol, quercetin and myricetin. In that region calculated and observed IR spectra of the studied flavonoids agree very well in wavenumbers and intensities what is an evidence that the chosen theoretical model (B3LYP/6-31 + G(d,p)) is quite an appropriate one. Below 1000 cm^{-1} the bands are superimposed over a rather broad band having maximum at around 600 cm^{-1}. The origin of such a background is likely due to water molecules (the same broad characteristic is evident in the IR spectrum of pyrogallol hydrate while it is absent in the spectrum of pyrogallol anhydrate [32]). The observed intensity distribution in IR spectra of flavonols is a fortunate circumstance and of practical importance because when studying interactions of flavonoids with lipids only the flavonoid IR bands above 1000 cm^{-1} can be observed with certainty.

Concerning interactions between flavonoids and lipids in membranes the main role is played by flavonoid hydroxyl groups and the phosphate groups of phospholipid molecules. However, due to the great affinity of the phosphate groups towards water, it is reasonably to assume that flavonoid lipid interactions is mediated by water. Up to seven water molecules are adsorbed around the phosphate groups in model systems mimicking phospholipid molecule with both the hydrogen atoms in the water molecule participating in hydrogen bonding [38]. At the same time it has been confirmed theoretically that phenol-water clusters with similar hydrogen-bonding pattern as in water clusters are equally stable [39].

Acknowledgments

The authors thank the Croatian Science Foundation [grant ref. IP-2016-06-8415] for financial support.

Conflicts of interest

None.

Appendix A. Supplementary data

Supplementary data to this article can be found online at https://doi.org/10.1016/j.saa.2017.11.057.

References

[1] S.V. Verstraeten, C.G. Fraga, P.I. Oteiza, Flavonoid–membrane interactions: consequences for biological actions, in: Cesar G. Fraga (Ed.), Plant Phenolics and Human Health: Biochemistry, Nutrition, and Pharmacology, John Wiley & Sons, Inc. 2010, pp. 107–135.
[2] K.E. Heim, A.R. Tagliaferro, D.J. Bobilya, Flavonoid antioxidants: chemistry, metabolism and structure-activity relationships, J. Nutr. Biochem. 13 (2002) 572–584.
[3] F. Ollila, K. Halling, P. Vuorela, H. Vuorela, J.P. Slotte, Characterization of flavonoid–biomembrane interactions, Arch. Biochem. Biophys. 399 (2002) 103–108.
[4] K. Cieslik-Boczula, J. Maniewska, G. Grynkiewicz, W. Szeja, A. Koll, A.B. Hendrich, Interaction of quercetin, genistein and its derivatives with lipid bilayer—an ATR IR spectroscopic study, Vib. Spectrosc. 62 (2012) 64–69.
[5] B. Pawlikowska-Pawlega, W.I. Gruszecki, L. Misiak, R. Padush, T. Piersiak, B. Zarzyka, J. Pawelec, A. Gawron, Modification of membranes by quercetin, a naturally occuring flavonoid, via its incorporation in the polar head group, Biochim. Biophys. Acta 1768 (2007) 2195–2204.
[6] B. Pawlikowska-Pawlega, L.E. Misiak, B. Zarzyka, R. Paduch, A. Gawron, W.I. Gruszecki, FTIR, ^{1}H NMR and EPR spectroscopy studies on the interaction of flavone apigenin with dipalmitoylphosphatidylcholine liposomes, Biochim. Biophys. Acta 1828 (2013) 518–527.
[7] Y. Yao, G. Lin, Y. Xie, P. Ma, G. Li, Q. Meng, T. Wu, Preformulation studies of myricetin: a natural antioxidant flavonoid, Pharmazie 69 (2014) 19–26.
[8] I.O. Protsenko, L.A. Bulavin, D.M. Hovorun, Investigation of Structural Properties of Quercetin by Quantum Chemistry Methods, WDS'10 Proceedings of Contributed Papers, Part III, 2010 51–54.
[9] Guang-Zhu Jin, Yuriko Yamagata, Ken-Ichi Tomia, Structure of quercetin dihydrate, Acta Cryst C46 (1990) 310–313.
[10] S. Domagała, P. Munshi, M. Ahmed, B. Guillot, C. Jelsch, Structural analysis and multipole modelling of quercetin monohydrate—a quantitative and comparative study, Acta Cryst B67 (2011) 63–78.
[11] T.Z. Todorova, M.G. Traykov, A.V. Tadjer, Zh.A. Velkov, Structure of flavones and flavonols. Part I: Role of substituents on the planarity of the system, Comput. Theor. Chem. 1017 (2013) 85–90.
[12] S. Aparicio, A systematic computational study on flavonoids, Int. J. Mol. Sci. 11 (2010) 2017–2038.
[13] N.F.L. Machado, L.A.E. Batista de Carvalho, J.C. Otero, M.P.M. Marques, A conformational study of hydroxyflavones by vibrational spectroscopy coupled to DFT calculations, Spectrochim. Acta A 109 (2013) 116–124.
[14] M.P. Waller, D.E. Hibbs, J. Overgaard, J.R. Hanrahan, T.W. Hambley, Flavone, Acta Crystallogr. E59 (2003) o767–o768.
[15] M.C. Etter, Z. Urbanczyk-Lipkowska, S. Baer, P.F. Barbara, The crystal structures and hydrogen-bond properties of three 3-hydroxy-flavone derivatives, J. Mol. Struct. 144 (1986) 155–167.
[16] M. Muresan-Pop, M.M. Pop, G. Borodi, M. Todea, T. Nagy-Simon, S. Simon, Solid dispersions of myricetin with enhanced solubility: formulation, characterization and crystal structure of stability-impeding myricetin monohydrate crystals, J. Mol. Struct. 1141 (2017) 607–614.
[17] J.M. Petroski, C. De Sa Valente, E.P. Kelson, S. Collins, FTIR spectroscopy of flavonols in argon and methanol/argon matrixes at 10 K. Reexamination of the carbonyl stretch frequency of 3-hydroxyflavone, J. Phys. Chem. A 106 (2002) 11714–11718.
[18] T. Teslova, C. Corredor, R. Livingstone, T. Spataru, R.L. Birke, J.R. Lombardi, M.V. Canamares, M. Leona, Raman and surface-enhanced Raman spectra of flavone and several hydroxyl derivatives, J. Raman Spectrosc. 38 (2007) 802–818.
[19] A. Vavra, R. Linder, K. Kleinermanns, Gas phase infrared spectra of flavone and its derivatives, Chem. Phys. Lett. 463 (2008) 349–352.
[20] J.M. Dimitrić Marković, Z.S. Marković, D. Milenković, S. Jeremić, Application of comparative vibrational spectroscopic and mechanistic studies in analysis of fisetin structure, Spectrochim. Acta A 83 (2011) 120–129.
[21] J.P. Cornard, J.C. Merlin, A.C. Boudet, L. Vrielynck, Structural study of quercetin by vibrational and electronic spectroscopies combined with semiempirical calculations, Biospectroscopy 3 (1997) 171–249.
[22] I.A. Adejoro, E. Akintemi, O.O. Adeboye, C. Ibeji, Quantum mechanical studies of the structure-activity relationship and electronic vibration of some dietary flavonoids, Asian J. Appl. Sci. 7 (2014) 117–128.
[23] D. Vojta, K. Dominković, S. Miljanić, J. Spanget-Larsen, Intramolecular hydrogen bonding in myricetin and myricitrin. Quantum chemical calculations and vibrational spectroscopy, J. Mol. Struct. 1131 (2016) 242–249.
[24] G. Baranović, Generalized harmonic mode scrambling, Chem. Phys. Lett. 271 (1997) 226–231.
[25] Gaussian 09, Revision D.01, M. J. Frisch, G. W. Trucks, H. B. Schlegel, G. E. Scuseria, M. A. Robb, J. R. Cheeseman, G. Scalmani, V. Barone, B. Mennucci, G. A. Petersson, H. Nakatsuji, M. Caricato, X. Li, H. P. Hratchian, A. F. Izmaylov, J. Bloino, G. Zheng, J. L. Sonnenberg, M. Hada, M. Ehara, K. Toyota, R. Fukuda, J. Hasegawa, M. Ishida, T. Nakajima, Y. Honda, O. Kitao, H. Nakai, T. Vreven, J. A. Montgomery, Jr., J. E. Peralta, F. Ogliaro, M. Bearpark, J. J. Heyd, E. Brothers, K. N. Kudin, V. N. Staroverov, T. Keith, R. Kobayashi, J. Normand, K. Raghavachari, A. Rendell, J. C. Burant, S. S. Iyengar, J. Tomasi, M. Cossi, N. Rega, J. M. Millam, M. Klene, J. E. Knox, J. B. Cross, V. Bakken, C. Adamo, J. Jaramillo, R. Gomperts, R. E. Stratmann, O. Yazyev, A. J. Austin, R.

Cammi, C. Pomelli, J. W. Ochterski, R. L. Martin, K. Morokuma, V. G. Zakrzewski, G. A. Voth, P. Salvador, J. J. Dannenberg, S. Dapprich, A. D. Daniels, O. Farkas, J. B. Foresman, J. V. Ortiz, J. Cioslowski, and D. J. Fox, Gaussian, Inc., Wallingford CT, 2013.
[26] E.E. Zvereva, A.R. Shagidullin, S.A. Katsyuba, Ab initio and DFT predictions of infrared intensities and Raman activities, J. Phys. Chem. A 115 (2011) 63–69.
[27] H. Yoshida, K. Takeda, J. Okamura, A. Ehara, H. Matsuura, A New Approach to vibrational analysis of large molecules by density functional theory: wavenumber-linear scaling method, J. Phys. Chem. A 106 (2002) 3580–3586.
[28] G. Fogarasi, Xuefeng Zhou, P.W. Taylor, P. Pulay, The calculation of ab initio molecular geometries: efficient optimization by natural internal coordinates and empirical correction by offset forces, J. Am. Chem. Soc. 114 (1992) 8191–8201.
[29] S. Califano, Vibrational States, John Wiley & Sons Ltd., 1976
[30] J.H. Schachtschneider, Vibrational Analysis of Polyatomic Molecules V, Technical Report No. 231-64, Shell Development Company, 1964.
[31] J.H. Schachtschneider, Vibrational Analysis of Polyatomic Molecules VI, Technical Report No. 57-65, Shell Development Company, 1965.
[32] D.E. Braun, R.M. Bhardwaj, J.-B. Arlin, A.J. Florence, V. Kahlenberg, U.J. Griesser, D.A. Tocher, S.L. Price, Absorbing a little water: the structural, thermodynamic, and kinetic relationship between pyrogallol and its tetarto-hydrate, Cryst. Growth Des. 13 (2013) 4071–4083.
[33] G. Keresztury, F. Billes, M. Kubinyi, T. Sundius, A. Density Functional, Infrared linear dichroism, and normal coordinate study of phenol and its deuterated derivatives: revised interpretation of the vibrational spectra, J. Phys. Chem. A 102 (1998) 1371–1380.
[34] D. Michalska, W. Zierkiewicz, D.C. Bienko, W. Wojciechowski, T. Zeegers-Huyskens, "Troublesome" vibrations of aromatic molecules in second-order Moller-Plesset and density functional theory calculations: infrared spectra of phenol and phenol-OD revisited, J. Phys. Chem. A 105 (2001) 8734–8739.
[35] W. Roth, P. Imhof, M. Gerhards, S. Schumm, K. Kleinermanns, Reassignment of ground and first excited state vibrations in phenol, Chem. Phys. 252 (2000) 247–256.
[36] J.M. Dimitrić Marković, Z.S. Marković, J.B. Krstić, D. Milenković, B. Lučić, D. Amić, Interpretation of the IR and Raman spectra of morin by density functional theory and comparative analysis, Vib. Spectrosc. 64 (2013) 1–9.
[37] M.M. Dias, N.F.L. Machado, M.P.M. Marques, Dietary chromones as antioxidant agents—the structural variable, Food Funct. 2 (2011) 595–602.
[38] R. Parthasarathi, V. Subramanian, N. Sathyamurthy, Hydrogen bonding in phenol, water, and phenol-water clusters, J. Phys. Chem. A 109 (2005) 843–850.
[39] D. Mishra, S. Das, S. Krishnamurthy, S. Pal, Understanding the orientation of water molecules around the phosphate and attached functional groups in a phospholipid molecule: a DFT-based study, Mol. Simul. 39 (2013) 937–955.